AMER. ZOOL., 41:1364–1374 (2001)

Feeding Motor Patterns in Anurans: Insights from Biomechanical Modeling[1]

ERIC S. MALLETT,[2,*] GARY T. YAMAGUCHI,* JAMES M. BIRCH,[3,†] AND KIISA C. NISHIKAWA[4,†]

*Department of Chemical, Bio and Materials Engineering, Arizona State University, Tempe, Arizona 85287-6006

†Department of Biological Sciences, Northern Arizona University, Flagstaff, Arizona 86011-5640

SYNOPSIS. During feeding in anurans, the mouth opens while the tongue, which is attached to the mandible at the front of the mouth, rotates forward. Due to the relative simplicity of its anatomy and the complexity of its motion, tongue protraction in frogs presents an ideal system for exploring the neural control of multijoint movements. In this study, we used a forward dynamic, rigid body model with four segments and two muscles to investigate open loop control of tongue protraction in the Australian white-lipped tree frog, *Litoria caerulea*. Model parameters include the mass distribution, initial position and initial angular velocity of each segment and the anatomy and physiology of each muscle. Model variables include the level of muscle activation at each time step and impulsive torques to open and close the mouth. The model gives X,Y coordinates of each segment and joint angles at each time step as output. The model was tested using scaled, normalized EMG signals and impulsive joint torques to predict the paths of the lower jaw tip and tongue tip. Predicted paths were compared to experimentally observed paths using Pearson product-moment correlation coefficients. Simulations demonstrate that the genioglossus muscles likely play a minor role, if any, in determining the trajectory of the tongue in most anurans. Most of the force for tongue protraction comes from angular momentum transferred to the tongue by the opening jaws. In anurans, tongue protraction is dynamically stable and will occur as long as the musculoskeletal elements are in the correct initial position.

INTRODUCTION

In many anuran species, feeding is a precise, target-oriented, prehensile movement that resembles human reaching in many respects. Specifically, both reaching and feeding require precise multijoint coordination such that the vectors of rotational movement at the joints sum to produce a nearly straight end-point trajectory (Nishikawa and Gans, 1996). In these species, tongue projection during feeding is also ballistic and like jumping (Lutz and Rome, 1994), requires high power output from the muscles and is planned in advance with no control after launch (Nishikawa, 1999).

In contrast to the arms of humans, the anatomy of the anuran tongue and jaws is relatively simple. Whereas arms and legs have more muscles than segments, the jaws and tongues of anurans are composed of relatively few muscles. Anurans generally possess a single depressor mandibulae muscle for opening the mouth, a complex of six adductor mandibulae muscles for closing the mouth, and two extrinsic muscles in the tongue (Magimel-Pelonnier, 1924; Horton, 1982; Regal and Gans, 1976). The m. genioglossus is involved in tongue protraction, whereas the m. hyoglossus is involved in tongue retraction (Nishikawa, 2000). Due to the relative simplicity of its anatomy and the complexity of its motion, tongue protraction in frogs presents an ideal opportunity for exploring the neural control of multijoint movement using a forward dynamic,

[1] From the Symposium *Motor Control of Vertebrate Feeding: Function and Evolution* presented at the Annual Meeting of the Society for Integrative and Comparative Biology, 3–7 January 2001, at Chicago, Illinois.

[2] Present address of Eric Mallett is 6462 Grayson Hills Drive NE, Rio Rancho, NM 87124.

[3] Present address of James Birch is Department of Integrative Biology, University of California, Berkeley, CA 94720.

[4] Corresponding author; e-mail: Kiisa.Nishikawa@nau.edu

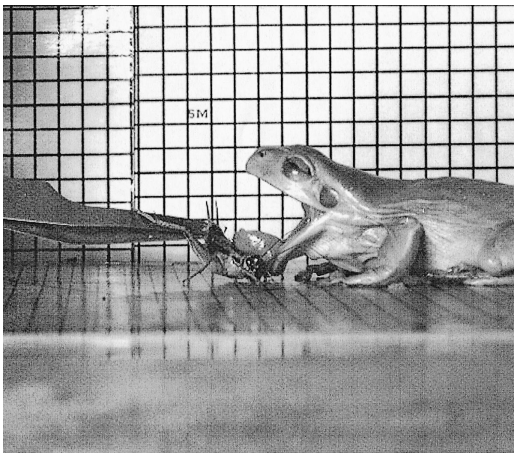

FIG. 1. Tongue protraction in the Australian white-lipped tree frog, *Litoria caerulea*. In *Litoria*, the anteriorly attached tongue rotates about the mandibular symphysis as the mouth is opened. The tongue shortens during protraction.

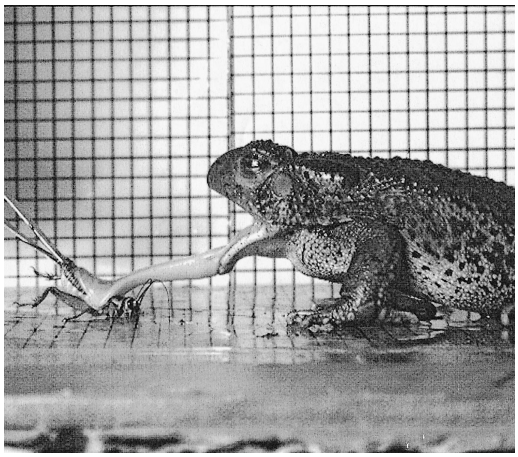

FIG. 2. Tongue protraction in Woodhouse's toad, *Bufo woodhousii*. In *Bufo*, the anteriorly attached tongue rotates about the mandibular symphysis as the mouth is opened. The tongue lengthens during protraction due to transfer of angular momentum from the opening mouth to the tongue.

rigid body model to simulate the kinematics of tongue protraction.

Recent studies have shown that anuran species exhibit at least three different, non-exclusive mechanisms of tongue protraction during feeding (Nishikawa, 2000). These are: 1) mechanical pulling (Fig. 1), in which the tongue shortens as the genioglossus muscle contracts, pulling the tongue pad forward over the mandibular symphysis; 2) inertial elongation (Fig. 2), in which the tongue lengthens during protraction due to transfer of angular momentum from the opening mouth to the tongue pad; and 3) muscular hydrostatic elongation (Fig. 3), in which the tongue lengthens due to the contraction of an intrinsic tongue muscle, m. genioglossus dorsoventralis, which translates a decrease in tongue thickness into an increase in tongue length (Nishikawa *et al.*, 1999). Although our long term goal is to model the evolution of frog tongues, we begin here with a model of a mechanical puller, the Australian white-lipped tree frog *Litoria caerulea* (Fig. 1).

During feeding in anurans, the mouth opens while the tongue, which is attached to the mandible at the front of the mouth, rotates forward over the mandibular symphysis. In the present study, we used a forward dynamic, rigid body model to investigate the open loop control of tongue protraction in *Litoria*.

MODEL DEVELOPMENT AND TESTING

Biomechanical models may use either an inverse or forward dynamic approach. In inverse dynamic models, the joint torques that must have acted at joints are inferred

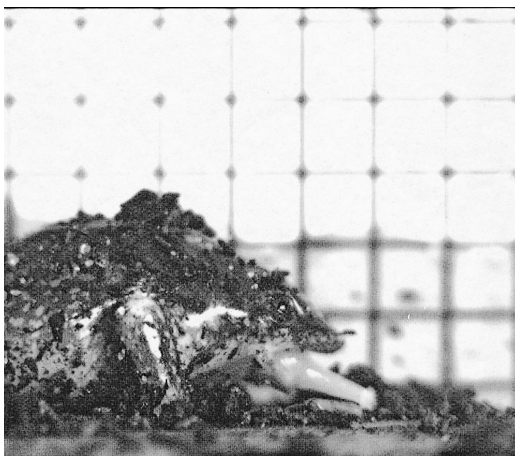

FIG. 3. Tongue protraction in the African pig-nosed frog, *Hemisus marmoratum*. In *Hemisus*, the tongue lengthens during protraction due the contraction of the m. genioglossus dorsoventralis, an intrinsic tongue muscle that translates a decrease in tongue thickness into an increase in tongue length.

from kinematic accelerations (*e.g.*, Bermejo and Ziegler, 1989). In contrast, forward dynamic models predict movement trajectories from the anatomy and physiology of the musculoskeletal system (Yamaguchi and Zajac, 1990). The predictions can then be tested with kinematic data. In general, forward dynamic models represent the neural computations associated with motor control more realistically than inverse dynamic models and require fewer assumptions (Yamaguchi *et al.*, 1995).

To study the dynamics of tongue protraction in anurans, a planar, forward dynamic musculoskeletal model was developed for a mechanical puller, *Litoria caerulea*. The model has four degrees of freedom and two muscles (Fig. 4). The muscles are the m. genioglossus and the m. hyoglossus. In the model, these muscles are used to actuate the tongue, whereas impulsive joint torques are applied at the proximal end of the lower jaw to open or close the mouth. Several anatomical features were not included in the model. In particular, the hyobranchium and mentomeckelian joint were omitted. The tongue pad rests on the hyobranchium, which is protracted and retracted during tongue protraction (Emerson, 1977). Most anurans also have a mentomeckelian joint within the mandible that flexes downward during mouth opening (Deban and Nishikawa, 1992).

Based upon the geometry of the jaws and tongue, the system was divided into four linked segments (Fig. 4). The most proximal segment represents the lower jaw and the remaining three segments represent the tongue. The locations of hypothetical ''joints'' within the tongue were chosen based upon tongue geometry. The most proximal segment of the tongue begins at the origin of the m. genioglossus and extends to the proximal end of the lingual sinus, the middle segment extends from the proximal to the distal end of the lingual sinus, and the distal segment extends from the distal end of the lingual sinus to the tongue tip. Neither the m. genioglossus nor the m. hyoglossus insert in the proximal segment, and both muscles have fibers that insert in the middle and distal segments. Adding more tongue segments would increase the complexity of the model without improving precision.

The parameters of the forward dynamic, rigid body model include: 1) the mass, center of mass, moment of inertia, initial position and initial angular velocity of each segment; 2) the origin, insertion, fiber length, thickness, physiological cross-sectional area, active force-length behavior, passive force-length behavior, rate of force development and force-velocity relationship of each muscle. Model variables include the level of muscle activation at each time step and impulsive torques to open and close the mouth. The model gives the X,Y coordinates of each segment and the joint angles at each time step as output.

The equations of motion for the musculoskeletal model were derived via Kane's method (Kane and Levinson, 1985). For a model with n degrees of freedom, the planar, dynamic equations of motion for the rigid-body model are as follows:

$$M\ddot{\vec{\theta}} = [\vec{T} + \vec{V} + \vec{G} + \vec{E}] \qquad (1)$$

where:

M = a [n × n] mass matrix that describes the mass distribution at time t;

$\ddot{\vec{\theta}}$ = a [n × 1] vector that contains the second time derivatives of n joint angles;

$\vec{T}$ = a [n × 1] vector of segmental torques;

$\vec{V}$ = a [n × 1] vector that describes the moment contributions of inertial forces;

$\vec{G}$ = a [n × 1] vector that describes the moment contributions of gravitational forces;

$\vec{E}$ = a [n × 1] vector that describes the moment contributions of external forces.

For the tongue muscles, joint torques were obtained using a lumped-parameter, Hill-type muscle model (Fig. 5) that consists of a damping element, a contractile element and a parallel elastic element which simulate muscle force-length and force-ve-

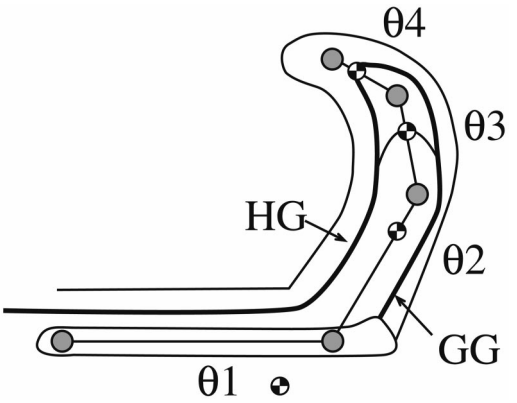

FIG. 4. Four degree of freedom, forward dynamic, rigid body model of the tongue and jaws of the white-lipped tree frog, *Litoria caerulea*. Segment 1 is the lower jaw and segments 2–4 are segments of the tongue. θ1–θ4 represent the joint angles. HG = hyoglossus muscle, GG = genioglossus muscle.

locity behavior, as well as muscle activation and contraction dynamics (Zajac, 1989). The damping element was assigned an arbitrarily high value to prevent oscillations, which are not observed *in vivo.* The force-length behavior of the parallel elastic element is given by:

$$\frac{F^{PE}}{F_o^M} = P_{po}\left\{\exp\left[\frac{1}{L_{po}}\left(\frac{L^M}{L_o^M} - 1\right)\right] - 1\right\} \quad (2)$$

where F^{PE} is the force generated by the parallel elastic element, F_o^M is the maximum isometric muscle force, L^M is the muscle length and L_o^M is the optimal muscle fiber length. Values of the variables P_{po} and L_{po} were chosen so that the shape of the curve (Fig. 6) matches the experimentally measured passive behavior of the genioglossus and hyoglossus muscles of *Litoria* (see Peters and Nishikawa, 1999). Time-dependent material behavior at extreme loading rates, while probably important in inertial elongators, was not included in the model.

The force generated by the contractile element is modeled as a multiplicative function of activation dynamics, isometric properties and isotonic behavior. This is expressed as:

$$F^M = a(t)ISOM(L^M)ISOT(V^M)F_o^M \quad (3)$$

where a(t) is the percentage of actively contracting muscle fibers, V^M is the muscle's

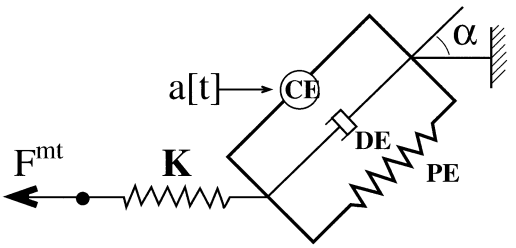

FIG. 5. Hill-type muscle model. F^{mt} = overall musculotendon force, K^t = tendon stiffness, a(t) = percent of active muscle fibers, CE = contractile element, DE = damping element, PE = parallel elastic element, and α = pennation angle.

lengthening or shortening velocity, and F_o^M is the muscle's maximum isometric force. The functions ISOM and ISOT are representations of the muscle's normalized isometric (Fig. 7) and isotonic (Fig. 8) behavior. The shapes of these curves are governed by equations 4 and 5:

$$\frac{F^M(L^M)}{F_o^M} = \begin{cases} \frac{1}{2}\left[1 - \cos\left(\frac{2\pi X_{pp}}{Pt_2 - Pt_1} - A_p + 1\right)\right] \\ \qquad 0.405 \le \frac{L^M}{L_o^M} \le 1.625 \\ 0.0 \qquad \text{elsewhere} \end{cases} \quad (4)$$

where

$$X_{pp} = \frac{L^M}{L_o^M} + \frac{B_p A_p^3}{\left(\frac{L^M}{L_o^M} - C_p\right)^2 + A_p^2}$$

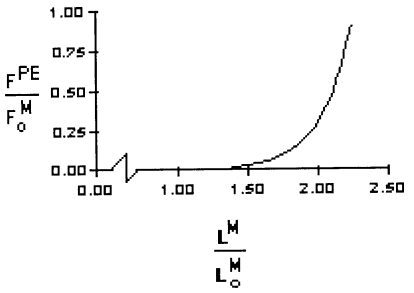

FIG. 6. Force–length behavior of the parallel elastic elements as described by Equation 2. The variables P_{po} and L_{po} were modified to match the passive behavior of the m. genioglossus and m. hyoglossus of *Litoria* (Peters and Nishikawa, 1999).

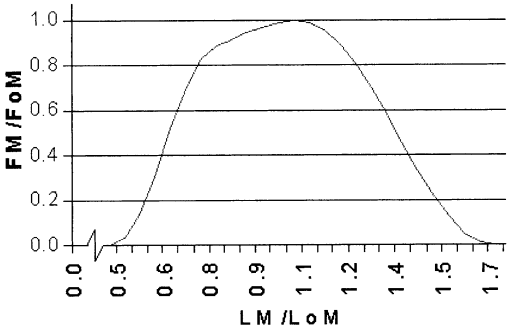

FIG. 7. Isometric force-length behavior of the contractile elements as described by Equation 4. The variables A_p, B_p and C_p were modified to match the isometric force-length behavior of the m. genioglossus and m. hyoglossus of *Litoria* (Peters and Nishikawa, 1999).

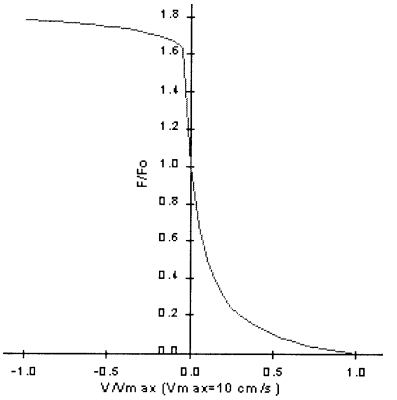

FIG. 8. Force–velocity behavior of the contractile elements as described by Equation 5.

$$\frac{F_{act}^{M}(V^{M})}{F_{o}^{M}} = \begin{cases} \dfrac{1 - \dfrac{V^{M}}{V_{max}}}{1 + \dfrac{V^{M}}{kV_{max}}}, & \dfrac{V^{M}}{V_{max}} \geq 0.0 \\ \dfrac{1}{A} \ln\left(\dfrac{\dfrac{V^{M}}{V_{max}} + B}{C}\right), & \dfrac{V^{M}}{V_{max}} < 0.0 \end{cases} \quad (5)$$

where values of the variables A_p, B_p, C_p, Pt_1, Pt_2, A, B, C, V_{max} and F_o^M were chosen to match the experimentally measured force-length behavior of the genioglossus and hyoglossus muscles (see Peters and Nishikawa, 1999). Because neither the genioglossus nor the hyoglossus muscle possesses a tendon, no model of tendon elasticity was required. In the model, we used a very short tendon with infinite stiffness.

Actuation of the musculoskeletal model occurs through 1) impulsive mouth opening and closing moments at the jaw joint; and 2) excitation-contraction dynamics of the tongue muscles. To simulate opening and closing of the mouth, impulsive joint torques were applied at a specific moment in time. For each trial, the timing and magnitude of the opening and closing torques were chosen to best match the observed jaw kinematics for that trial. For each trial, only one impulsive opening torque and one impulsive closing torque were applied at the jaw joint. In the forward dynamic model, these torques not only open and close the mouth but also propagate to the tongue and thus affect the kinematics of tongue protraction.

For the tongue muscles, activation dynamics were modeled as follows:

$$\frac{dA}{dt} = -A[k_2 + k_1 C(t)] + (k_2 + k_1 - k_2 A_{min})C(t) + k_2 A_{min} \quad (6)$$

where k_1, k_2 and A_{min} are muscle specific constants. The function C(t) models the neural input to the muscles and is based on experimentally measured electromyographic data. The rectified experimental EMG signal is low-pass filtered with a cut-off frequency in the range of 3 to 7 Hz. The resulting waveform is then normalized to the maximal occurring value, such that all values are between 0 and 1. Normalization allows for scaling of the C(t) profile. Scaling is required because the maximal level of muscle excitation is unknown. During computer simulations, the scaling factor for each muscle is varied until the best fit to the kinematic data is found.

The model was tested by using the scaled, normalized EMG signals and impulsive joint torques to predict the paths of the lower jaw tip and tongue tip. The predicted paths of the lower jaw and tongue tip were compared to the experimentally

observed paths using Pearson product-moment correlation coefficients.

MEASUREMENT OF MUSCLE ACTIVATION AND MOVEMENT KINEMATICS

For practical reasons, we chose to model tongue protraction in the white-lipped tree frog, *Litoria caerulea*, a pelomedusine hylid from Australia. Simulations were based on data collected from three individuals of *Litoria caerulea*, ranging from 20.3 to 37.9 g in body mass. Two to three trials were simulated for each individual. After videotaping 2–3 feeding trials for each individual with simultaneous electromyography, the frogs were sacrificed. For each individual frog, the mass and center of mass of each segment was measured. Moments of inertia for the proximal segment were calculated as for a wedge, and for the distal segments as for a cylinder. For each muscle, the origin, insertion, fiber length, thickness and physiological cross sectional area were measured. The passive and active force-length behavior and the rate of force development of each muscle were based on measurements from the m. genioglossus and m. hyoglossus of *Litoria* (Peters and Nishikawa, 1999). The force-velocity relationship has not yet been measured for these muscles and was assumed to be similar to that of vertebrate skeletal muscle in general.

Feeding behavior was videotaped at room temperature (21–25°C) with simultaneous electromyography. Waxworms (*Galleria* sp.) were used as prey and were placed at a distance of approximately 5 cm from the frog. A Display Integration Technologies model DIT 660 high-speed, multiframing video camera was used to film the frogs at 120 fields/sec with synchronized stroboscopic illumination. Kinematic analysis of feeding behavior follows Nishikawa and Roth (1991) and Deban and Nishikawa (1992). In each video field, the X,Y coordinates of the prey item, a nonmoving reference point, and several points on the head were digitized from the video monitor. The digitized points included: (1) the tip of the upper jaw; (2) the jaw joint; (3) the tip of the lower jaw; and (4) the tongue tip. The locations of all digitized points were measured with the jaw joint at the origin (0,0). The X,Y coordinates of the lower jaw tip and tongue tip, and the gape angle were measured in each video field.

Electromyographic recordings of muscle activity were obtained using bipolar, enamel-coated, stainless steel electrodes with a bared tip length of 1 mm. Electrodes were implanted percutaneously into the muscles of anesthetized subjects using 23–25 gauge hypodermic needles. The signals were amplified 1,000 times and recorded on an A. R. Vetter 8-channel FM tape recorder. Analog EMG signals were converted to digital data using a Datatran 50 kHz A/D conversion board, Peak Performance Technologies A/D acquisition software, and Run Technologies Data-Pac II waveform and signal processing software. The analog-to-digital conversion was performed at a sampling rate of 10 kHz. The digital signal was bandpass filtered with a pass band of 300 to 3,000 Hz. The filtered waveform was rectified and the average baseline noise subtracted. Electrodes were placed in the bellies of the m. genioglossus, m. hyoglossus, m. depressor mandibulae, and m. adductor mandibulae posterior longus.

Pearson product-moment correlation coefficients were used to compare the experimental data, obtained from digitized feeding sequences, to the movements predicted by the model. For each simulation, the X,Y coordinates of the lower jaw tip and tongue tip, and the gape angle were compared at each time step (8.33 msec).

SIMULATION RESULTS

Forward dynamic simulations of a model with four degrees of freedom represents a fairly formidable problem. To achieve a model with realistic tongue and jaw movement, it was first necessary to approximate normal jaw movements. Once a realistic gape profile was achieved, it was relatively straightforward to achieve realistic tongue motion. However, this required that the tongue shortens initially as the m. genioglossus contracts. If the tongue doesn't shorten during the initial stages of tongue protraction, then its moment of inertia is too large. The result is that the mouth fails to open completely and the tongue accordions onto itself instead of unfolding.

TABLE 1. *R-squared values from seven simulations of tongue protraction in* Litoria caerulea *(Pearson product-moment correlation).*

Individual	Trial	Gape angle	Lower jaw		Tongue	
			X	Y	X	Y
L-1	1	0.84	0.81	0.87	0.42	0.69
	2	0.96	0.92	0.97	0.97	0.83
L-2	1	0.95	0.83	0.98	0.42	0.95
	2	0.90	0.77	0.93	0.56	0.99
L-3	1	0.99	0.99	0.99	0.90	0.11
	2	0.91	0.99	0.99	0.01	0.80
	3	0.89	0.52	0.85	0.65	0.79

The model demonstrates that a two impulse mouth opening and closing torque profile explains the observed gape angle profile with a relatively high degree of accuracy. The r^2 values ranged from 0.84 to 0.99 (Table 1). The model also does a fairly good job of predicting the horizontal (r^2 = 0.52–0.99) and vertical (r^2 = 0.85–0.99) position of the lower jaw over time. For each trial, single impulsive torques acting at a specified time were used to simulate mouth opening and closing. The magnitude of the opening torque ranged from −345 to −585 g cm sec^{-2}, and the time of activation ranged from 0.4 to 10 msec. The magnitude of the closing torque ranged from 271 to 549 g cm sec^{-2}, and the time of activation ranged from 15 to 35 msec. On one hand, the good fit between the simulation and the observed kinematics is not surprising because the timing and magnitude of the torques was chosen to match the observed gape profile. On the other hand, it is somewhat surprising that such a simple model of mouth opening and closing, with open loop control and a single impulsive torque for each, does such a good job of predicting mouth opening in most trials (Table 1).

It is interesting to note that, if the mouth closing torque is not included in the model, then both jaw and tongue paths deviated significantly from the experimental data. The jaw path deviates because braking of mouth opening by the mouth closing torque is an important feature of the gape profile. The tongue path deviates because the change in direction of the jaw acceleration imparts significant angular momentum to the tongue pad, which helps to propel the tongue out of the mouth.

It is also interesting to note that there was significant variation among the trials of a single individual in how well the model predicted the gape angle and the position of the lower jaw tip. For example, for individual L-3, the r^2 values for the X and Y coordinates of the lower jaw tip were 0.99 in the first two trials, but were 0.52 and 0.85, respectively, in the third trial. These results suggest that, although the neural control of the mm. depressor and levator mandibulae during mouth opening in *Litoria* is well predicted by simple open-loop control, it is likely that the level of recruitment of individual muscles may vary from trial to trial within an individual.

The model performs less well in explaining the horizontal (r^2 = 0.01–0.97) and vertical (r^2 = 0.11–0.99) position of the tongue tip, although the model performs well in at least some trials (*i.e.*, Individual L-1, trial 2, Table 1). In general, the model performed better at predicting the Y-position of the tongue tip than at predicting the X-position, and it performed better at predicting tongue tip position for L-2 than for L-1 or L-3. In all cases in which the model performs less well in predicting feeding kinematics, the movements are somewhat more complex in the animals than in the simulations (Fig. 9). The more complex shape of the experimental jaw and tongue tip paths probably reflects online feedback correction in the animals, which was not included in the model.

An interesting result of the simulations is that the genioglossus muscle is ten times too small to affect the trajectory of the tongue tip. To investigate model sensitivity, the activity of the genioglossus muscle was scaled over a range of 0–100, well beyond the maximum value of 1 allowed by normalization. The activity of the genioglossus muscle had a negligible effect on tongue tip path below a scaling factor of 10. When the activity of the genioglossus muscle was scaled to 0, the tongue tip path was unchanged. In contrast, when the activity of the genioglossus muscle was scaled high enough to affect the tongue trajectory, the

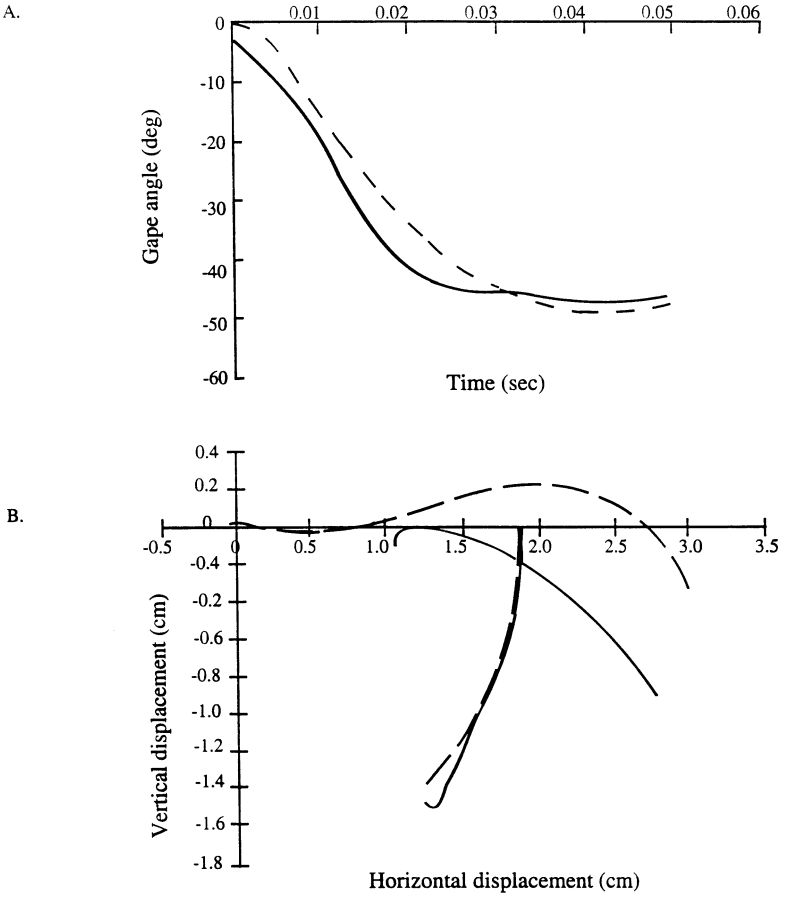

FIG. 9. Simulation results for individual L-1, trial 2 (see Table 1). Solid lines represent experimental data and dashed lines represent simulated data. A. Gape angle *vs.* time (r^2 = 0.96). The experimental gape angle profile is more complex than the simulated gape angle profile. B. Experimental and simulated paths of the lower jaw tip (below, more vertical path) and tongue tip (above, more horizontal path) in the X,Y plane. There is a good fit between the experimental and simulated lower jaw tip paths (r^2 = 0.92 and 0.97 for X and Y, respectively). The fit between the experimental and simulated tongue tip paths is not as good, especially in the vertical dimension (r^2 = 0.97 and 0.83 for X and Y, respectively).

resulting tongue movement was difficult to control.

This result suggests that the motion of the tongue during feeding is dynamically stable. The mouth opening torque produced by the m. depressor mandibulae causes the tongue pad to move upward due to its inertia. Transfer of angular momentum from the lower jaw to the tongue propels the tongue pad over the symphysis and onto the prey. This result is unlikely to be an artifact of the model for several reasons. First, the physiological cross-sectional area of the genioglossus muscle is in fact very small. In *Litoria*, it is 4–5 times smaller than that of the hyoglossus muscle. Secondly, the parameters of the muscle model were chosen to match values measured empirically for *Litoria* by Peters and Nishikawa (1999).

In fact, muscle stimulation experiments in toads (*Bufo marinus*) have found that supramaximal stimulation of the genioglossus muscle is not sufficient to produce tongue protraction (Emerson, 1977; Gans and Gorniak, 1982; Nishikawa and Gans, 1992). These studies are consistent with the simulation results and support the hypothesis that the genioglossus muscles are too small to affect the tongue trajectory in *Litoria*.

This result leaves us with the question of

the role that the genioglossus muscles play during prey capture. At least three non-exclusive functions are possible. First, contraction of the genioglossus muscles pulls the tongue mass closer to the symphysis, reducing the force required to flip the tongue out of the mouth. Second, shortening of the tongue also reduces the moist contact area between the tongue and the buccal floor, thus reducing the surface tension between them. Third, contraction of the genioglossus muscles aids tongue protraction by changing the moment of inertia of the tongue pad.

DISCUSSION

The results of the simulations demonstrate that, in general, a four degree of freedom, forward dynamic, rigid body model predicts the gape angle and the X,Y position of the lower jaw tip very well in most trials. The X,Y position of the tongue tip is predicted reasonably well at least in some trials. It is somewhat surprising that the rigid body model works as well as it does in predicting tongue position, given that the tongue itself is not a rigid body and has no joints. We conclude that the muscular hydrostatic shape changes that the tongue undergoes during protraction are not critical for predicting the location of the tongue in the X,Y plane. Likewise, the anatomical details that were lacking in the model, including forward movement of the hyoid and bending of the mandibles, are not critical for simulating tongue protraction. However, because the forward movement of the hyoid affects the fiber length of the hyoglossus muscle, it might be more important in a model of tongue retraction.

Forward dynamic models underscore the amount of information that is necessary to predict the kinematics of movement. For each segment, it is necessary to measure the mass, center of mass, moment of inertia, initial position and initial angular velocity. For each muscle, it is necessary to measure the origin, insertion, fiber length, thickness and physiological cross-sectional area. In addition, it is necessary to specify the active and passive force-length behavior, the rate of force development and the force-velocity relationship for each muscle. Finally, one needs to know the level of muscle activation at each time step from electromyography. In our model, all variables except the force velocity relationships were measured for the genioglossus and hyoglossus muscles of *Litoria*. The model also demonstrates that open loop control without feedback does a reasonably good job at predicting tongue and jaw movement. Although the fit between experimental and simulated data would undoubtedly be improved by adding feedback to the model, the fit is remarkably good without such feedback.

The results also underscore the value of using a forward dynamic versus inverse dynamic model to study the neural control of movement. In forward dynamic models, forces generated at any given joint are propagated to all other joints. In contrast, joint torques are inferred from kinematic accelerations in inverse dynamic models. Our use of a forward dynamic model was absolutely critical in understanding the role of interjoint coordination during tongue protraction in *Litoria*. Because we used a forward dynamic model, we were able to demonstrate that more than 90% of the force of tongue protraction comes from angular momentum transferred to the tongue by the opening jaws. Less than 10% of the force comes from the contraction of the genioglossus muscles themselves. Had we used an inverse dynamic approach, we would have inferred a large joint torque from the kinematic data, but would have been unable to resolve whether the force was generated by the m. genioglossus *vs.* transferred to the tongue by the opening jaws.

The model demonstrates that tongue protraction in *Litoria* is dynamically stable. In other words, the observed movement will occur, without feedback control, as long as the musculoskeletal elements are in the correct initial position. Increasingly, a variety of complex movements have been found to exhibit dynamic stability. For example, an open loop, dynamic model of a running cockroach was found to resist a variety of perturbations in the horizontal plane without any feedback control (Kubow and Full, 1999). The stability of the model comes from the mechanical relationship of the leg

joints, although the particular aspects of leg morphology and force production that contributed to stability remain unknown. Similarly, control of the anuran tongue is achieved largely through its mechanical relationship with the lower jaw. It is not necessary for the central nervous system to perform either complex open loop multijoint coordination or to provide feedback control. In fact, what the nervous system must do is provide neural input to the muscles that does not interfere with the mechanically stable movement.

For us, an important question is whether or not this model of tongue protraction in a mechanical puller, *Litoria caerulea*, can be extended to other anuran species, particularly species like toads which use inertia to elongate their tongues during ballistic tongue protraction (Nishikawa, 1999). In fact, there are relatively few differences in the anatomy of the feeding apparatus between *Litoria* and *Bufo* (Nishikawa, 2000). Our current hypothesis is that the major differences between mechanical pullers like *Litoria* and inertial elongators like *Bufo* are in the velocity of mouth opening (hence in the transfer of angular momentum from the opening mouth to the tongue) and in the amount and orientation of epimysial connective tissues surrounding the genioglossus muscles. Fewer collagen fibers in general, and fibers oriented at angles greater than 54°44″ relative to the long axis of the tongue (Kier and Smith, 1985), will facilitate elongation of the tongue upon transfer of angular momentum from the opening jaws (Nishikawa, 2000; Zepnewski and Nishikawa, 2000).

If our hypothesis is correct, then the results from this model should apply to *Bufo* and other inertial elongators as well. In fact, the physiological cross-sectional area of the genioglossus muscles is proportionally even smaller in *Bufo* than in *Litoria* because the muscle is relatively less massive and the fibers are longer. Thus, the genioglossus muscle likely contributes little to tongue protraction in *Bufo* as well.

In summary, simulations of tongue protraction using a forward dynamic, rigid body model demonstrate that the genioglossus muscles likely play a minor role, if any, in determining the trajectory of the tongue in most anurans. Most of the force for tongue protraction comes from angular momentum transferred to the tongue from the opening jaws. These results are consistent with experiments demonstrating that stimulation of the genioglossus muscle is not sufficient for protracting the tongue (Emerson, 1977; Gans and Gorniak, 1982). On the other hand, muscle denervation experiments show that no protraction occurs without contraction of the genioglossus muscles (Nishikawa and Gans, 1992, 1996), suggesting that they may play some other critical role, such as breaking wet adhesion between the tongue and the buccal floor, shifting the tongue mass forward, and/or overcoming the inertia of the tongue pad. Tongue projection is dynamically stable in anurans and will occur as long as the musculoskeletal elements are in the correct initial position.

ACKNOWLEDGMENTS

This research was supported by grants from the National Science Foundation (IBN-9809974 to KCN and BES-9257395 to GTY) and the National Institutes of Health (R25-GM56931 to KCN). We thank Philip Service and Kristopher Lappin for helpful comments on earlier versions of the manuscript.

REFERENCES

Bermejo, R. and H. P. Ziegler. 1989. Prehension in the pigeon. II. Kinematic analysis. Exp. Brain Res. 75:577–585.

Deban, S. M. and K. C. Nishikawa. 1992. The kinematics of prey capture and the mechanism of tongue protraction in the green tree frog, *Hyla cinerea*. J. Exp. Biol. 170:235–256.

Emerson, S. B. 1977. Movement of the hyoid in frogs during feeding. Amer. J. Anat. 149:115–120.

Gans, C. and G. C. Gorniak. 1982. Functional morphology of lingual protrusion in marine toads (*Bufo marinus*). Amer. J. Anat. 163:195–222.

Horton, P. 1982. Diversity and systematic significance of anuran tongue musculature. Copeia 1982:595–602.

Kane, T. R. and D. A. Levinson. 1985. *Dynamics: Theory and applications.* McGraw-Hill, New York.

Kier, W. M. and K. K. Smith. 1985. Tongues, tentacles and trunks: The biomechanics and movement of muscular hydrostats. Zool. J. Linn. Soc. 83:207–324.

Kubow, T. M. and R. J. Full. 1999. The role of the mechanical system in control: A hypothesis of

self-stabilization in hexapedal runners. Phil. Trans. R. Soc. London Ser. B 354:849–861.

Lutz, G. J. and L. C. Rome. 1994. Built for jumping: The design of the frog muscular system. Science 263:370–372.

Magimel-Pelonnier, O. 1924. La langue des Amphibiens. Thése, Fac. Sci. Paris. A. Saugnac et E. Provillard, Bordeaux.

Nishikawa, K. C. 1999. Neuromuscular control of prey capture in frogs. Phil. Trans. Roy. Soc. London, Biol. Sci. 354:941–954.

Nishikawa, K. C. 2000. Feeding in frogs. *In* K. Schwenk (ed.), *Feeding: Form, function and evolution in tetrapod vertebrates*, pp. 117–147, Academic Press, San Diego, California.

Nishikawa, K. C. and C. Gans. 1992. The role of hypoglossal sensory feedback during feeding in the marine toad, *Bufo marinus*. J. Exper. Zool. 264: 245–252.

Nishikawa, K. C. and C. Gans. 1996. Mechanisms of prey capture and narial closure in the marine toad, *Bufo marinus*. J. Exp. Biol. 199:2511–2529.

Nishikawa, K. C. and G. Roth. 1991. The mechanism of tongue protraction during prey capture in the frog *Discoglossus pictus*. J. Exp. Biol. 159:217–234.

Nishikawa, K. C., W. M. Kier, and K. K. Smith. 1999. Morphology and mechanics of tongue movement in the African pig-nosed frog (*Hemisus marmoratum*): A muscular hydrostatic model. J. Exp. Biol. 202:771–780.

Peters, S. E. and K. C. Nishikawa. 1999. Comparison of isometric contractile properties of the tongue muscles in three species of frogs, *Litoria caerulea*, *Dyscophus guinetti* and *Bufo marinus*. J. Morphol. 242:107–124.

Regal, P. J. and C. Gans. 1976. Functional aspects of the evolution of frog tongues. Evolution 30:718–734.

Yamaguchi, G. T. and F. E. Zajac. 1990. Restoring unassisted natural gait to paraplegics with functional neuromuscular stimulation: A computer simulation study. IEEE Trans. Biomed. Eng. 37:886–902.

Yamaguchi, G. T., D. W. Moran, and J. Si. 1995. A computationally efficient method for solving the redundant problem in biomechanics. J. Biomechanics 28:999–1005.

Zajac, F. E. 1989. Muscle and tendon: Properties, models, scaling and application to biomechanics and motor control. CRC Critical Reviews in Biomechanical Engineering 17:359–411.

Zepnewski, E. and K. C. Nishikawa. 2000. Connective tissue in ballistic tongues. J. Morphol. 248:304.